

## Article

# Experimental Research on the Dynamic Characteristics of Several Model Soils in Small Strain Range and Application in Shaking Table Model Test

Zhaoxia Ma <sup>1</sup>, Guobo Wang <sup>2</sup> and Yao Wang <sup>2,\*</sup><sup>1</sup> Department of Architecture and Material Engineer, Hubei University of Education, Wuhan 430205, China<sup>2</sup> College of Civil Engineering and Architecture, Wenzhou University, Wenzhou 325035, China

\* Correspondence: 20461542029@stu.wzu.edu.cn

**Abstract:** Reasonable model soil is very important in shaking table model tests to reduce the distortion of the soil structure stiffness ratio. Several model soils, such as sawdust soil, sawdust sand, rubber granular soil, rubber powder soil, and sawdust kaolin were prepared and a dynamic triaxial test proceeded to determine their dynamic characteristics. The experimental results showed that the variation of the dynamic shear modulus and dynamic damping ratio with dynamic shear strain was consistent with that of undisturbed soil. Finally, sawdust soil was adapted to a shaking table test of complex interaction systems and achieved good results. The results showed that sawdust soil is feasible as model soil. The research results can provide helpful references for the design of a similar shaking model test.

**Keywords:** model soil; sawdust soil; sawdust sand; dynamic characteristics; resonance column test; shaking table test



**Citation:** Ma, Z.; Wang, G.; Wang, Y. Experimental Research on the Dynamic Characteristics of Several Model Soils in Small Strain Range and Application in Shaking Table Model Test. *Buildings* **2023**, *13*, 592. <https://doi.org/10.3390/buildings13030592>

Academic Editor: Wusheng Zhao

Received: 8 February 2023

Revised: 19 February 2023

Accepted: 22 February 2023

Published: 23 February 2023



**Copyright:** © 2023 by the authors. Licensee MDPI, Basel, Switzerland. This article is an open access article distributed under the terms and conditions of the Creative Commons Attribution (CC BY) license (<https://creativecommons.org/licenses/by/4.0/>).

## 1. Introduction

Existing earthquake damage shows that the damage to underground structures during earthquakes is mainly imposed on the underground structures by the surrounding soil layers [1]. As a result, the characteristics of the surrounding soil layer have a decisive influence on the seismic response of underground structures, and this influence is mainly reflected by the soil structure stiffness ratio [2].

The shaking table model test is a powerful method to study the dynamic interaction between soil and underground structures. To make the model test reflect the seismic response law of underground structures reasonably, the selection of model soil in the model test is of utmost significance. In the model test of underground structures, structures are generally made of particulate concrete [3], plexiglass [4], aluminum alloy [5], and gypsum [6]. Compared with the original concrete material, the elastic modulus of these materials and the stiffness of the structure are much weaker than the original structure. Therefore, the soil structure stiffness ratio of the model soil to the model structure is quite different from that of the original soil to the prototype structure if the prototype soil is still used in the model test. This will lead to the distortion of the soil-structure stiffness ratio similarity ratio, by which the response of the structural model cannot truly reflect the response of the prototype structure. To reduce the distortion of the stiffness ratio, the model soil needs to be reconfigured, instead of using the original soil. On the other hand, the load capacity of the early constructed shaking table is limited [3,6], and the sum of the weights of the model box and model soil will exceed its load capacity easily. Sawdust soil, sawdust sand, rubber granule soil, and other remolded soil can be employed as model soil to overcome the above two problems. First, the density of the model soil can be reduced to meet the bearing capacity requirements of the shaking table. In addition, the model soil

with different shear modulus can be obtained by adjusting the content of sawdust, which can effectively reduce the distortion of the soil structure stiffness ratio.

Because of the above advantages, many scholars have conducted research on model soil. Kitada [7] performed a shaking table test in which silicone rubber was used to study the dynamic interaction between buildings during an earthquake. Turan [8] mixed bentonite, glycerol, and water to make model soil for the shaking table test to check the effectiveness of a laminar soil container. The model soil was prepared by mixing kaolin, bentonite, F-grade fly ash, lime, and water. The shear wave velocity of the model soil under different curing periods was tested by the bending element test. The undrained shear strength of the model soil was measured by the dynamic triaxial test, and model soil satisfying the test requirements was obtained [9–11]. Pistolas [12] studied the effects of rubber content and rubber particle size on the dynamic properties of rubber granular soil. El-Sherbiny [13] studied the dynamic characteristics of a mixture of sand and EPS at small stress and small strain. Yan [14] mixed sawdust and sand in a certain proportion to prepare sawdust for the shaking table test based on a similar theory.

Based on the above literature review, it can be seen that there is much work on model soil composed of silicone rubber and kaolin, but sawdust soil has been seldom studied. Before preparing the shaking table model test of the underground structure-soil-surface structure complex interaction system [15], we compared and selected the model soil. Considering the applicability and convenience of model soils, five kinds of model soils—sawdust soil, sawdust sand, rubber granular soil, rubber powder soil, and sawdust kaolin—were selected as the research objects, and a laboratory soil dynamic test was carried out. The dynamic characteristics of the test data were analyzed, and a reasonable model soil was selected.

## 2. Preparation of Model Soil

The main materials selected in this experiment were rubber particles, rubber powder, sawdust, kaolin, 0.2–0.8 mm quartz sand, and undisturbed silty clay. The materials are shown in Figure 1. The undisturbed silty clay was taken from a subway station site. Its moisture content was 20.4% and its density was 1.94 g/cm<sup>3</sup>. The sawdust was taken from a wood processing plant, and the rubber particle size was 2–4 mm. The rubber powder (40–60 mesh), quartz sand (0.2–0.8 mm), and kaolin (800 mesh) were purchased from the relevant factories. First, the silty clay was dried, rolled, and screened for particle sizes less than 3 mm. Similarly, sawdust was dried first and screened for impurities. In addition, the silty clay was mixed with sawdust, rubber particles, or rubber powder in a certain proportion, and the sawdust and kaolin were mixed to prepare the model soil.

Based on the existing literature [14] and preliminary tests, three different ratios were selected for each of the five model soils. For each model soil of the matching ratio, the density of the model soil was measured by the cutting ring method, and the water content of the model soil was measured. The contents of the obtained model soil are listed in Tables 1–5.

**Table 1.** Group A: sawdust + undisturbed soil (sawdust soil).

Group	Sawdust: Undisturbed Soil: Water	Density (g/cm <sup>3</sup> )	Sample No.
A1	1.00: 3.50: 1.70	1.30	A11 A12 A13
A2	1.00: 3.75: 2.50	1.33	A21 A22 A23
A3	1.00: 4.00: 2.50	1.40	A31 A32 A33

**Table 2.** Group B: rubber powder + undisturbed soil (rubber powder soil).

Group	Rubber Powder: Undisturbed Soil: Water	Density (g/cm <sup>3</sup> )	Sample No.
B1	1.00: 0.75: 0.74	1.30	B11 B12 B13
B2	1.00: 1.00: 0.62	1.40	B21 B22 B23
B3	1.00: 1.25: 0.66	1.45	B31 B32 B33

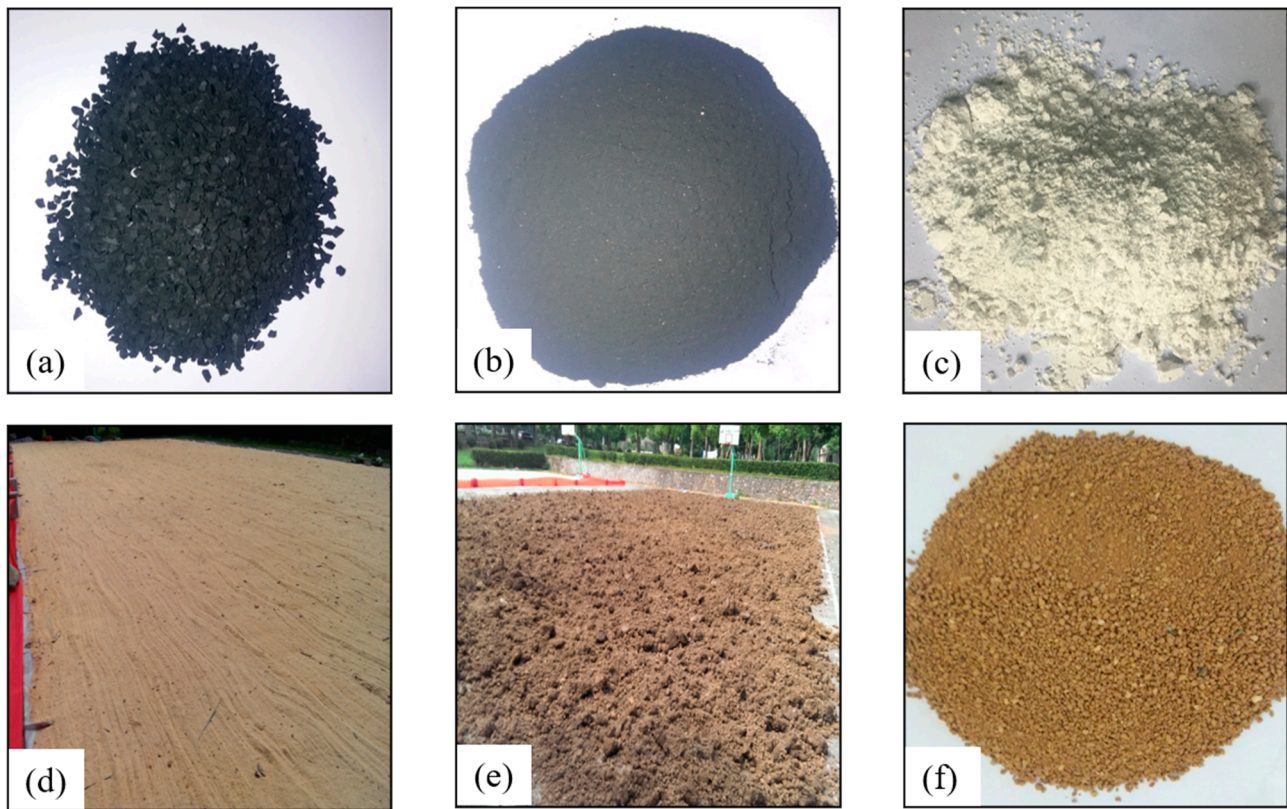


**Figure 1.** Model soil preparation material: (a) Rubber particle (2–4 mm), (b) Rubber powder (40–60 mesh), (c) Kaolin (80 mesh), (d) Drying of sawdust, (e) Drying of undisturbed soil, (f) Undisturbed silty clay powder.

**Table 3.** Group C: rubber particles + undisturbed soil (rubber granular soil).

Group	Rubber Particles: Undisturbed Soil: Water	Density (g/cm <sup>3</sup> )	Sample No.
C1	1.00: 0.75: 0.28	1.30	C11 C12 C13
C2	1.00: 1.00: 0.34	1.40	C21 C22 C23
C3	1.00: 1.50: 0.52	1.45	C31 C32 C33

**Table 4.** Group D: 0.2–0.8 mm quartz sand + sawdust (sawdust sand).

Group	Quartz Sand: Sawdust: Water	Density (g/cm <sup>3</sup> )	Sample No.
D1	2.00: 1.00: 3.02	1.05	D11 D12 D13
D2	2.50: 1.00: 2.94	1.10	D21 D22 D23
D3	3.00: 1.00: 3.09	1.15	D31 D32 D33

**Table 5.** Group F: sawdust Kaolin (sawdust Kaolin).

Group	Sawdust: Kaolin: water	Density (g/cm <sup>3</sup> )	Sample No.
F1	1.00: 3.50: 2.59	1.33	F11 F12 F13
F2	1.00: 3.75: 2.66	1.35	F21 F22 F23
F3	1.00: 4.00: 2.88	1.35	F31 F32 F33

Note: The model soil ratio is the mass ratio.

Regarding the above-mentioned matching ratio, the clay and the selected material were poured into a basin to be uniformly stirred. Then, water was poured in three times, and the mixture was uniformly stirred. Next, the mixture was layered into a split mould [16] and compacted in layers. The prepared test sample is shown in Figure 2.

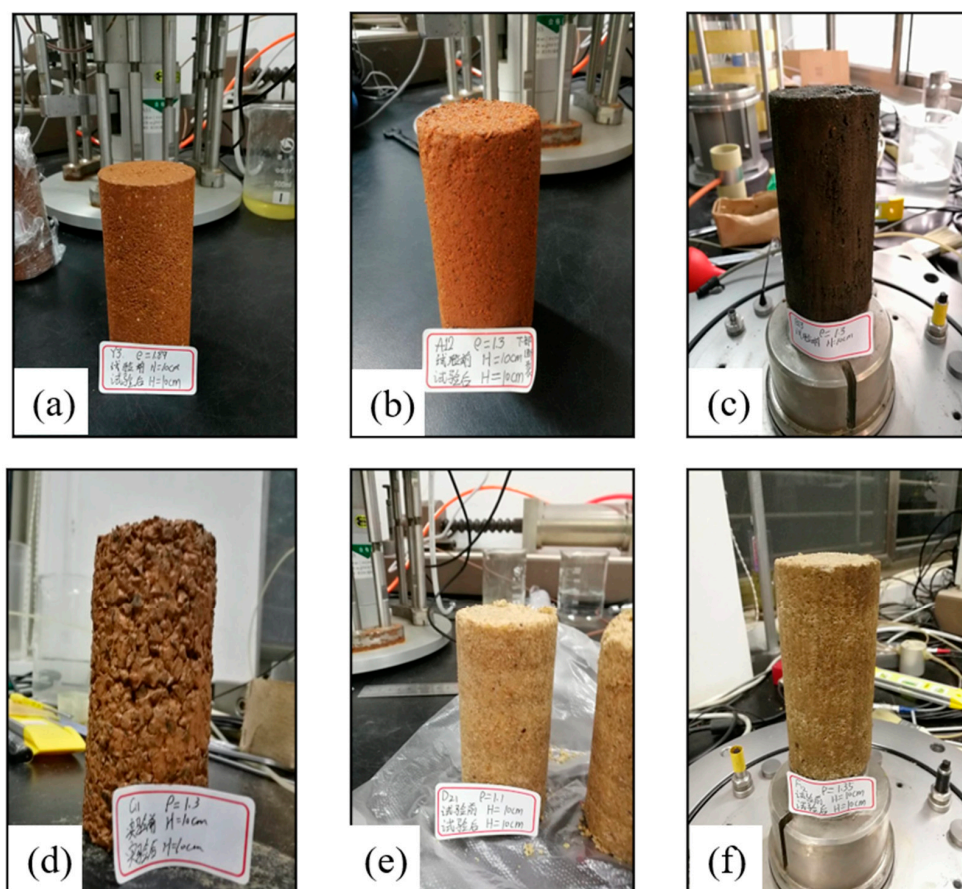


**Figure 2.** Original soil and model soil samples prepared: (a) Undisturbed soil, (b) Sawn soil sample, (c) Rubber powder soil, (d) Soil sample of rubber (e) Sawdust sand and soil, (f) Sawdust kaolin sample.

### 3. Test Instrument and Principle

Both dynamic triaxial and resonance column tests were carried out to determine the dynamic characteristics of the model soils. The main technical indicators for the dynamic triaxial test were as follows: geometric dimensions of the sample:  $39.1 \times 100$  mm (diameter  $\times$  height); vertical excitation frequency: 0.01–5 Hz; axial static/dynamic load: 0–40 kN; confining pressure: 0–1700 kPa; maximum volume change: 200 mL; resolution: 0.04 mL. With the vertical displacement sensor, the range was more than 50 mm, the accuracy was 0.07%, and the resolution was 0.208 m.

During the resonance column test, the lower end of the sample was fixed, and torque was generated by a driving system at the upper end of the sample. The response of the sample after excitation was measured by the acceleration sensor located on the top disk of the free end of the sample. In the process of resonance, the resonance frequency of the sample was measured by changing the frequency of the applied excitation. By the measured resonance frequency and the density and size of the specimen, the dynamic shear modulus was calculated. The damping ratio of the specimen under this shear strain was measured by free vibration.

For the resonance column test, the variation curves of dynamic shear strain and dynamic shear modulus of the soil samples can be obtained directly in a small strain range. However, the relationship between the axial force and axial strain of soil samples can be obtained in a large strain range by the dynamic triaxial test. We obtained the relationship between the dynamic shear strain and dynamic shear modulus of soil samples using a previously described treatment method [16]. To correlate the results of the dynamic triaxial test and the resonance column test, the dynamic elastic modulus  $E_d$  and the dynamic axial

strain  $\varepsilon_d$  were converted into the dynamic shear modulus  $G_d$  and the dynamic shear strain  $\gamma_d$  using Equations (1) and (2), respectively.

$$G_d = \frac{E_d}{2(1 + \mu_d)} \quad (1)$$

$$\gamma_d = \varepsilon_d(1 + \mu_d) \quad (2)$$

where  $\mu_d$  is the dynamic Poisson's ratio. Considering that the strength of the remolded soil is relatively low and the dynamic Poisson's ratio is difficult to determined based on the measured and empirical methods, the connection effect of the experimental data of the resonant column and the dynamic three-axis was very poor. Considering the aim of this study was to find a reasonable model soil for shaking table test to obtain the seismic response of the underground structure, the soil-structure stiffness ratio was a very important factor, and the stiffness of the soil was generally characterized by its shear modulus. Therefore, soil stiffness was determined in this study based on soil initial shear modulus, which were obtained by the resonant column test in the small strain range. Therefore, only the results of the resonant column test and the correlation analysis are given in this study.

#### 4. Dynamic Test Results

It is well known that the strength of model soils is lower than that of the original soil. The model soil samples will be damaged under higher confining pressures. Therefore, the model soil samples were only tested under confining pressures of 50 kPa and 100 kPa, while the original soil samples were tested under confining pressures of 50 kPa, 100 kPa, 200 kPa, and 300 kPa. It can be seen from Table 1 that the three soil samples were prepared in the shown proportions, and the average values of the three tests were taken from the test results.

#### 5. Discussion and Analysis of the Test Results

By the dynamic shear modulus of the undisturbed soil, the curves of the normalized dynamic shear modulus, and the dynamic damping ratio relative to the initial dynamic shear modulus with the dynamic shear strain (Figure 3), the typical softening effect of soft soil can be seen; that is, the soil shear modulus decreased with an increase in dynamic shear strain, and the damping increased with an increase in dynamic shear strain, which was consistent with a large number of research results on soft soil. Furthermore, the stress-strain relationship can be described by the classical Hardin–Drnevich model [17,18] or an improved Davidenkov model [19].

$$\frac{G_d}{G_{\max}} = 1 - \left[ \frac{(\gamma_d/\gamma_r)^{2B}}{1 + (\gamma_d/\gamma_r)^{2B}} \right]^A \quad (3)$$

$$\frac{\lambda}{\lambda_{\max}} = \left( 1 - \frac{G_d}{G_{\max}} \right)^\beta \quad (4)$$

where  $G_d$  and  $G_{\max}$  are the instantaneous dynamic shear modulus and the maximum shear modulus of soil, respectively;  $\lambda$  and  $\lambda_{\max}$  are the instantaneous damping ratio and maximum damping ratio, respectively;  $\gamma_d$  is the dynamic shear strain;  $\gamma_r$  is the shear strain for reference; and  $A$ ,  $B$ , and  $\beta$  are the calibration constants.

Figures 4–8 demonstrate the dynamic test results of five kinds of remolded soils; the following can be concluded:

1. The remolded soil satisfied the law of strain softening. The larger the surrounding rock was, the larger the initial dynamic shear modulus of the model soil was, and the slower the attenuation rate was. The damping ratio increased with increasing shear strain as a whole; however, the increase rate under different confining pressures was irregular.

2. The stiffness (initial dynamic shear modulus) of the five model soils under the same confining pressure was reduced as follows: rubber powder soil, sawdust sand, sawdust soil, rubber granular soil, and sawdust kaolin.

3. The content of the undisturbed soil in the soil sample was large; therefore, the dynamic shear modulus was large, which is a logical result.

4. Compared with the original soil, the shear modulus of sawdust soil was greatly reduced. In addition to sawdust kaolin and sawdust sand, the damping ratio of other soil samples increased to a certain extent; the main reason for this was that compared with the original soil, the remolded soil was loose and easy to consume because of the addition of elastic materials such as sawdust. Therefore, the damping ratio was relatively high, while the sawdust sand and sawdust kaolin were relatively dense because of quartz sand and kaolin, and the damping ratio did not increase but slightly decreased.

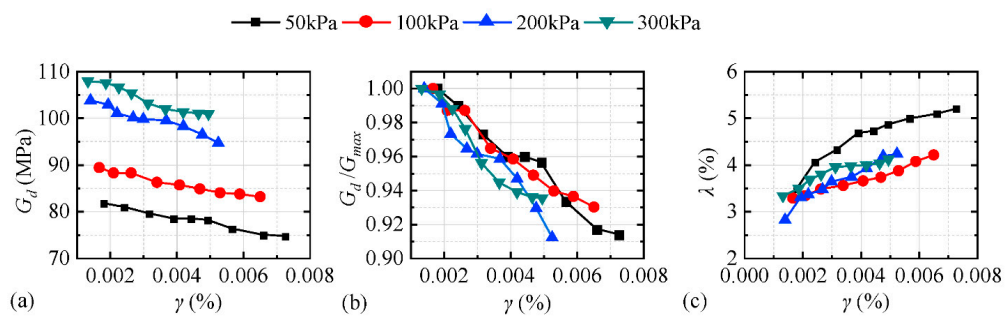


**Figure 3.** Test results of undisturbed soil: (a) Dynamic shear modulus curve of undisturbed soil, (b) Dynamic shear modulus curve of undisturbed soil is normalized, (c) Undisturbed soil dynamic damping ratio curve.

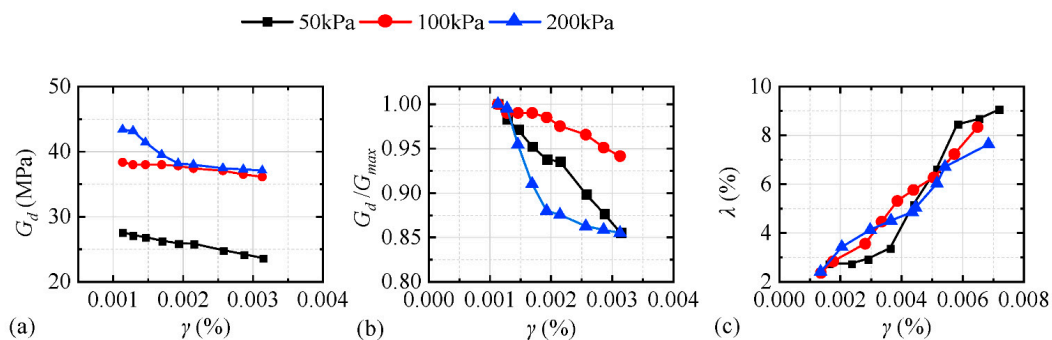


**Figure 4.** Test results of sawdust-soil: (a) Dynamic shear modulus curve of sawdust soil, (b) Normalized dynamic shear modulus curve of sawdust soil, (c) Curve of the dynamic damping ratio of sawdust soil.

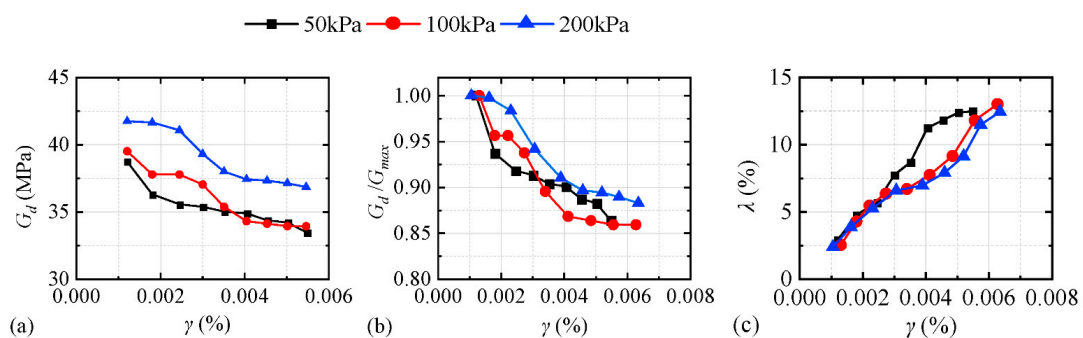


**Figure 5.** Test results of rubber powder soil: (a) Dynamic shear modulus, (b) Normalized dynamic shear modulus, (c) Dynamic damping ratio.

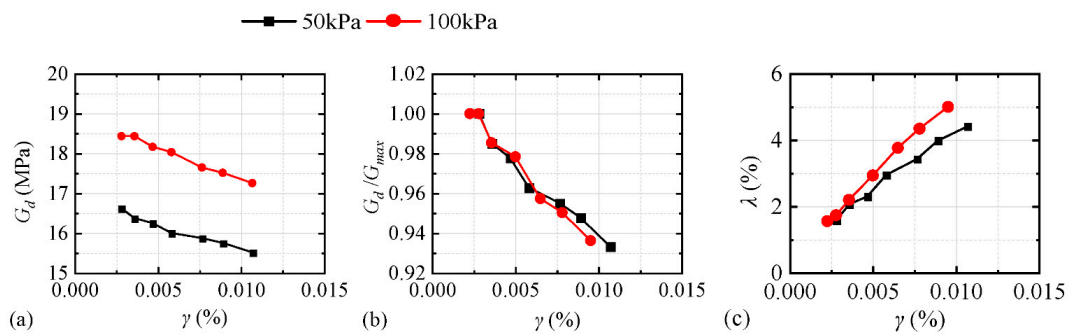


**Figure 6.** Test results of rubber granular soil; (a) Dynamic shear modulus (b) Normalized dynamic shear modulus, (c) Dynamic damping ratio.

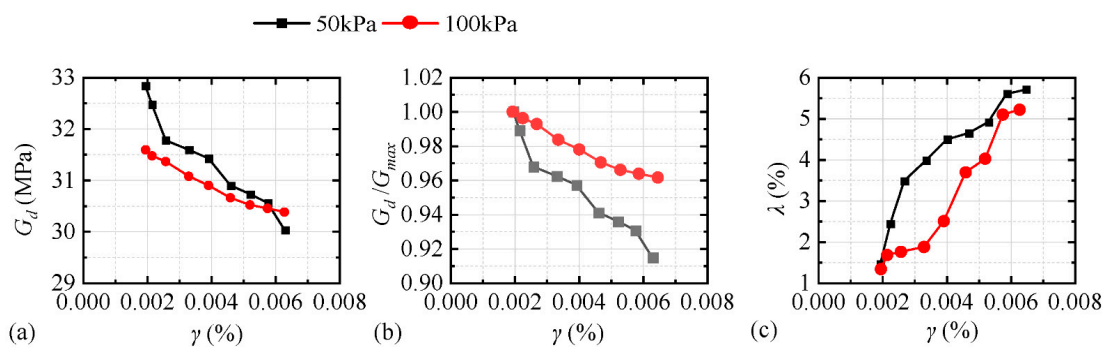


**Figure 7.** Test results of sawdust sand: (a) Dynamic shear modulus, (b) Normalized dynamic shear modulus, (c) dynamic damping ratio.

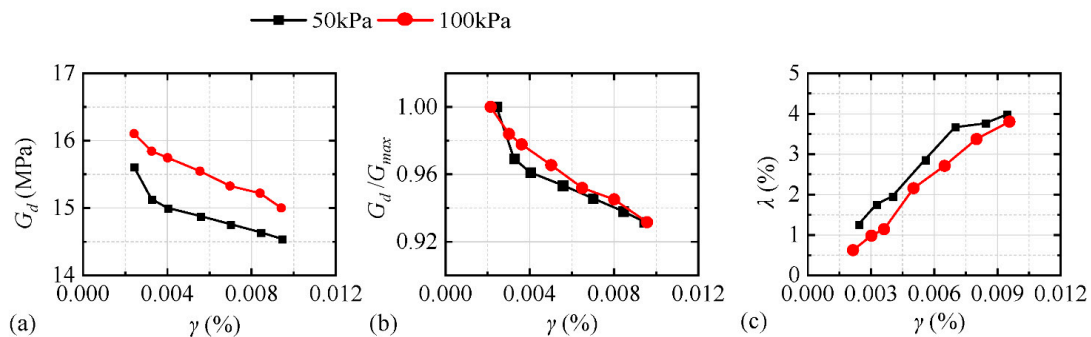


**Figure 8.** Test results of sawdust kaolin: (a) Dynamic shear modulus curve of sawdust kaolin, (b) Normalized dynamic shear modulus, (c) Dynamic damping ratio.

When the confining pressures were 50 kPa and 100 kPa, the dynamic characteristics of the five model soils and the undisturbed soils were compared. Figures 9 and 10 illustrate the curves of the variations in the dynamic shear modulus and the dynamic damping ratio with the dynamic shear strain, respectively. In general, the dynamic shear modulus attenuation law and the dynamic damping ratio of the five model soils were similar to those of the undisturbed soil and could be used as model soil for the model test. However, the effect of sawdust soil and sawdust sand was the best. The second was rubber granular soil, and the effect of the rubber powder soil and sawdust kaolin was the worst. The reason was that the main body of the sawdust soil and the sawdust sand was cohesive soil and quartz sand, which mainly embodied the mechanical properties of the soil, and the rubber powder and the kaolin had small particle sizes.

Therefore, the mechanical property was different from that of the original clay. In addition, rubber granular soil, because of the large elastic characteristics of rubber particles, leads to a large rebound of soil samples and is difficult to compact. At the same time,

because of the disadvantages of light mixing and easy floating, it is difficult to use rubber granular soil in a large volume. Based on the above-mentioned comparative analysis, it was suggested that sawdust and sawdust sand be used as model soil to perform the vibration table model test.

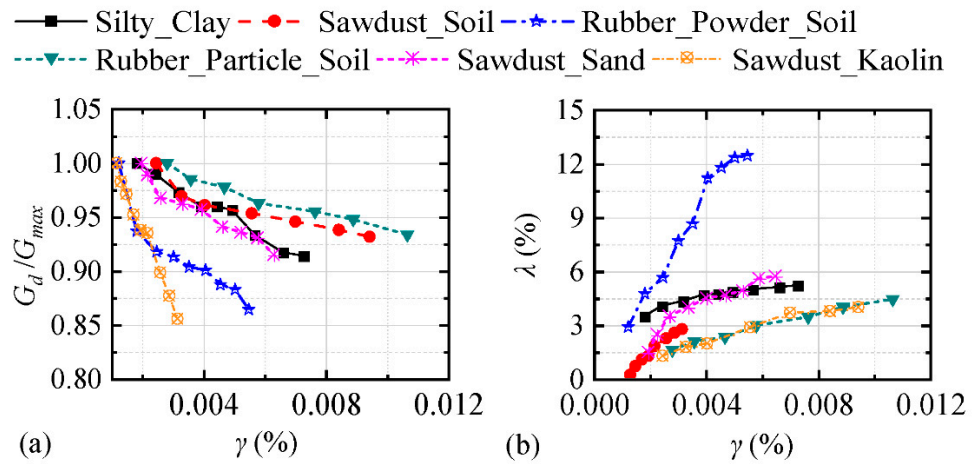


**Figure 9.** Comparison curve of dynamic characteristics between undisturbed soil and five models when confining pressure was 50 kPa: (a) Normalized dynamic shear modulus, (b) Dynamic damping ratio.

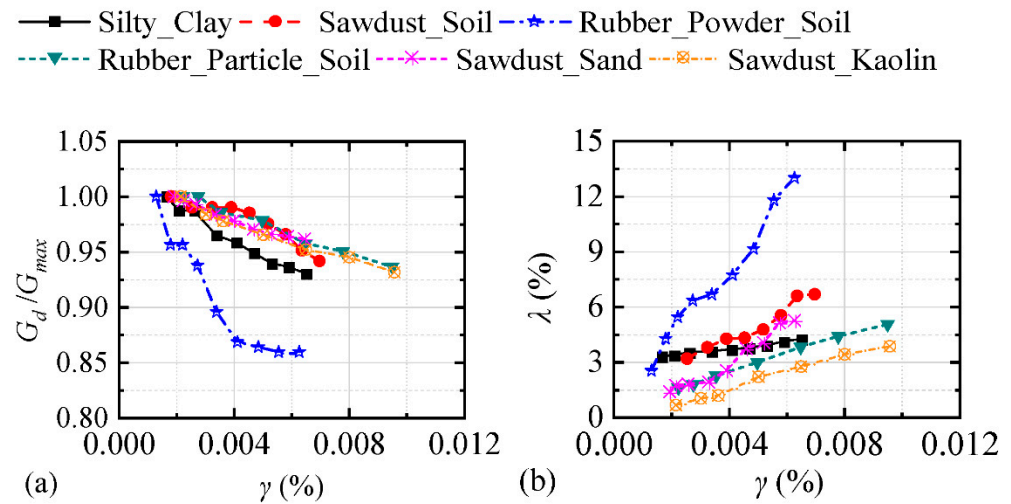


**Figure 10.** Comparison curve of dynamic characteristics between undisturbed soil and the five model soils when confining pressure was 100 kPa: (a) Normalized dynamic shear modulus, (b) Dynamic damping ratio.

### 6. Similarity Ratio Design of Soil-Structure Stiffness Ratio

Wang [2] provided the analytical equations for calculating the Stiffness Ratio of Tunnel—Soil (SRTS) of a circular tunnel (Equation (5)) and single hole rectangular tunnel (Equation (6)).

$$SRTS = \frac{6E_t I_t (1 + \nu_s)}{E_s (1 - \nu_t^2) R^3} \quad (5)$$

$$SRTS = \frac{6E_t I_t (1 + \nu_s)}{E_s (1 - \nu_t^2) R^3} \quad (6)$$

where  $E_t$  and  $E_s$  are the elastic modulus of the soil and the tunnel structure, respectively;  $\nu_s$  and  $\nu_t$  are Poisson’s ratio of soil and tunnel structure materials, respectively;  $R$  is the radius of the tunnel structure, and  $I_t$  is the moment of inertia of the unit width of the tunnel section,

which is equal to  $T^3/12$ .  $T$  is the wall thickness of the structure.  $H$  and  $L$  are the height and width of the rectangular tunnel structure, respectively, and  $I_B$  and  $I_H$  are the moment of inertia of the top (bottom) plate and the moment of inertia of the side wall, respectively.

For a typical circular tunnel, the diameter was 6 m and the segment thickness was 0.35 m. It was made of C30 concrete, had a soil mass density of  $1900 \text{ kg/m}^3$ , a shear modulus of 81.67 MPa when the confining pressure was 50 kPa, and a Poisson's ratio of 0.42. However, the structural model adopted the conventional geometric similarity ratio of 1/30, and the elastic modulus of unconventional particulate concrete was about 9.00 GPa. Thus, the similarity ratio of elastic modulus was 0.30, and the acceleration similarity ratio was 1. The prototype structure-soil stiffness ratio calculated according to the above formula was 6.58. To make the model structure-model soil similarity ratio of the model structure equal to or close to 1, the shear modulus of the model soil was set to 24.50 MPa.

For a typical single-cell rectangular tunnel, the length and width of the concrete section were 6 m, the wall thickness of the structure was 0.35 m, and C30 was used. The material and design of the soil parameters and structural model were consistent with the above results. Given the above formula, the stiffness ratio of the prototype structure to soil was 13.71. To make the similarity ratio of the model structure to the model soil equal to or close to 1, the shear modulus of the model soil was 24.50 MPa.

Compared with the test results of the above five model soils, it can be seen that the dynamic shear modulus of the sawdust soil was the closest to the theoretical calculation value when the confining pressure was 50 kPa, and the second was the sawdust sand (31.59 MPa). Therefore, the above suggestions were verified; that is, it is recommended that sawdust and sawdust sand be used as the model soil for the model test of the vibration table.

## 7. Model Test Verification

Yan [14] successfully used sawdust to study the seismic response of the raised immersed tube tunnel under non-uniform vibration excitation. Based on the test results of the above model soil, the shaking table test of the complex interaction system between underground structure, soil, foundation, and surface structure was carried out using sawdust soil [15] to explore the interaction between the underground structure and surface structure during an earthquake. The contents of this test included a free field test, soil-tunnel test, soil-surface frame test, and tunnel-soil-surface frame test. To verify the rationality of the sawdust soil, we only provided the results of the free field test conditions; the other conditions can be found in the literature [15].

Because of the large volume of sawdust soil, the undisturbed soil and sawdust were first dried on the site and then mixed and stirred in proportion (Figure 11a), filling, and layered compaction (Figure 11b). After stratified compaction, the soil surface was sealed and statically set for three days.

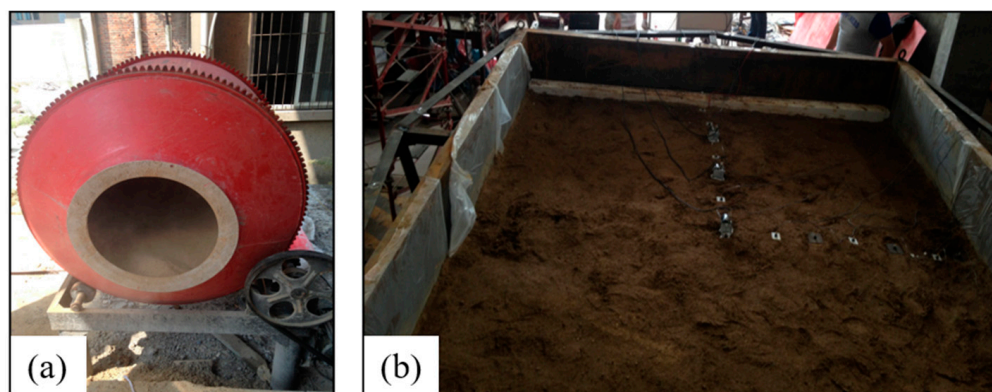


**Figure 11.** Stirring and filling of sawdust soil: (a) Sawdust soil stirring, (b) The sawdust soil is filled in the model box.

The depth of the soil at the free field was 1 m, and the arrangement of the acceleration sensor is shown in Figure 12.

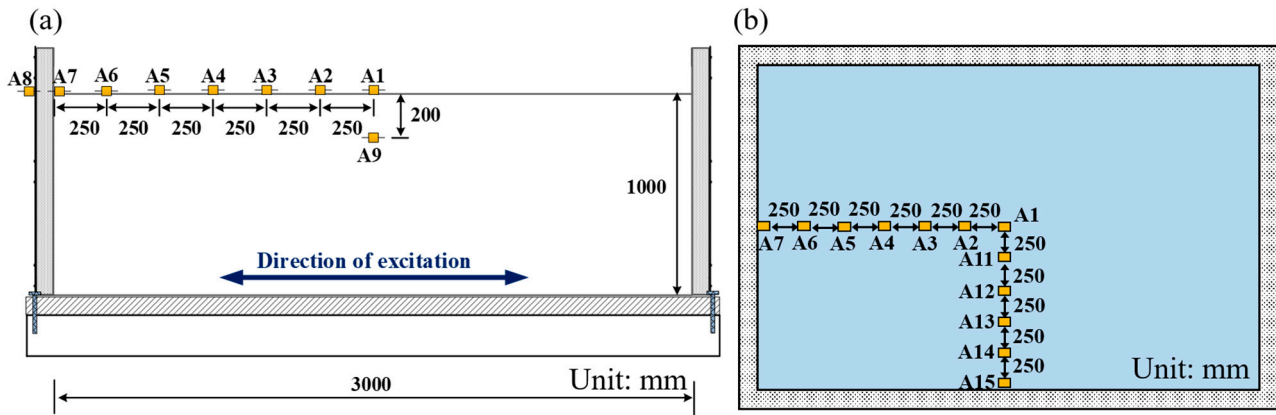


**Figure 12.** Layout of the free-field vibration table test sensor: (a) Schematic of the layout of the sensor: elevation, (b) Schematic diagram of the layout of the sensor: plane.

Taking the acceleration time history curve of the model soil surface under sinusoidal excitation as an example, the acceleration amplitude spectrum curve (Figure 13) was obtained by fast Fourier transform, and then, the frequency and damping ratio of the system was obtained by half power method [20,21] (Table 6).

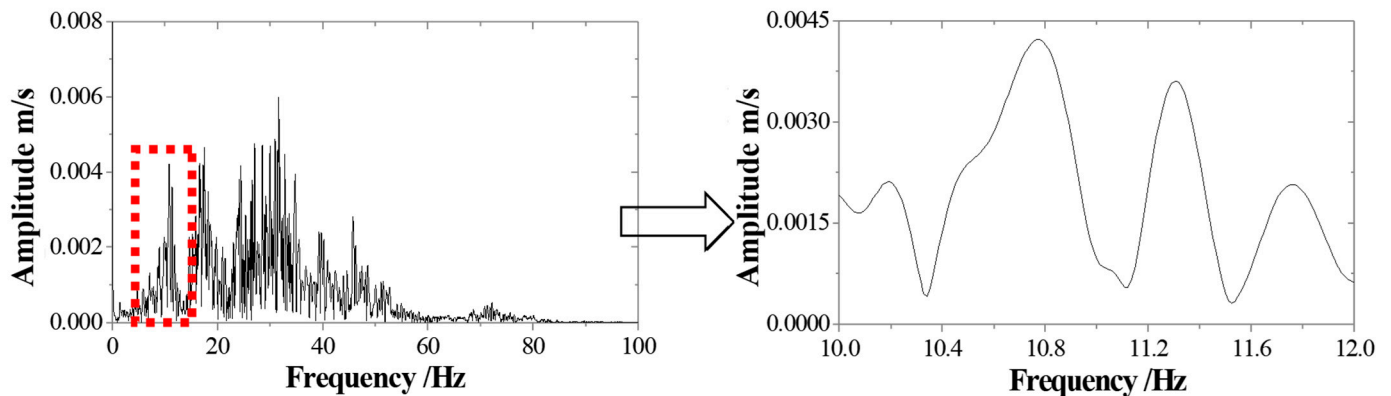


**Figure 13.** Acceleration peak spectrum curve at point A1 for the case of sinusoidal excitation.

**Table 6.** Identified system frequency and damping ratio.

Operating Mode	SIN5	SIN10
Frequency (Hz)	10.8	10.1
Damping ratio (%)	1.7	2.1

Note: The working conditions such as SIN5 can be found in Ref. [15].

The theoretical value of the natural vibration frequency of the model was obtained from the empirical Equation (7) of the free-field seismic response analysis:

$$f_n = (2n - 1)V_s / 4h \tag{7}$$

where  $f_n$  is the n-order natural vibration frequency of soil and  $V_s$  and  $h$  are shear wave velocity and soil thickness, respectively. As the density of sawdust soil is known, the shear wave velocity can be determined if the maximum dynamic shear modulus of sawdust soil is known, and the theoretical value of the natural vibration frequency of model soil can be determined.

The depth of the test soil was 0.9 m, and the overburden pressure at the average depth of 0.45 m was approximately 5.4 kPa, which was limited because of the limitation of the test instrument and could not be tested at such a small confining pressure. Therefore, the maximum dynamic shear modulus and circumference were considered to be the linear trend, and the value of the maximum dynamic shear modulus under different confining pressures of sawdust is shown in Figure 4a. The empirical formula of the relationship between confining pressure and initial shear modulus can be fitted based on the existing different confining pressure test data. The corresponding shear modulus at a lower confining pressure (especially low confining pressure that the test equipment cannot reach) can be determined according to this formula. This method can be called the epitaxial method. When the confining pressure of 5.4 kPa was determined, the maximum dynamic shear modulus could be approximately determined as 3.52 MPa by the epitaxial method, the shear wave velocity  $V_S$  was 54.42 m/s, and the theoretical value of the first-order natural frequency of model soil was  $54.4/4/0.9 = 15.10$  Hz. By comparing the experimental data with the theoretical calculation results, the following results were obtained:

1. The identified system frequency value of 10.80 Hz was close to the theoretical calculation value of 15.10 Hz. The reason for the error was that, when the soil-making power test was performed, the model soil was formed in a sample preparation device for convenience for the indoor test. A certain pressure was applied to the soil sample to make the soil sample compact. Thus, by comparison with the model soil in the model box, the compactness of the soil sample in the laboratory test was higher, so the fundamental frequency of the system was less than the laboratory test value. In future shaking table tests, the bending element can be used to directly measure the shear wave velocity in the model soil to reduce the influence of sampling disturbances.

2. With the increase of the amplitude of the input ground motion, the frequency of identification decreased and the damping increased, which indicated that the stiffness of soil was decaying, i.e., nonlinear deformation of soil occurred, which was consistent with the dynamic characteristics of soft soil.

Based on the above analysis, it can be preliminarily determined that the fundamental frequency of the model soil was 10.80 Hz, the corresponding shear wave velocity was 39.96 m/s, and the density was 1190 Kg/m<sup>3</sup>. Then, the dynamic shear modulus was 1.91 MPa. In this experiment, the size of the circular tunnel was consistent with that of the tunnel structure in Section 5; however, the tunnel was made of plexiglass with a density of 1120 kg m<sup>3</sup> and an elastic modulus of 2.10 GPa. The prototype structure-soil stiffness ratio was 6.58 according to Equations (5) and (6), and the structural-soil stiffness ratio of the structural model was only 4.03.

The structure-soil stiffness ratio of the prototype and the model was not equal to 1, and there was still a certain gap between both the prototype and the model. The main reason was that the thickness of the model soil (sawdust soil) was too thin, the soil was relatively loose, and its stress level was low, which also showed that in the complex design of the soil-structure interaction shaking table model test, it was impossible to achieve all aspects, and only the main factors could be grasped. The structure-soil stiffness similarity ratio distortion could only be reduced as much as possible and perhaps it could not be completely avoided.

## 8. Conclusions

In this study, five types of model soil were prepared based on the undisturbed silty clay and common additive materials, and the dynamic characteristics of soils were given. Based on their respective dynamic characteristics, some suggestions on the selection of model soil were given, the suggestions were applied to the shaking table model test of the complex interaction system, and good results were obtained. The main research results of this paper were as follows:

1. The variation of dynamic shear modulus and dynamic damping ratio of various model soils with dynamic shear strain agreed well with that of undisturbed soil, which

showed that the model soil could reflect the dynamic characteristics of the undisturbed soil, and could be used in the model test instead of the undisturbed soil, and had the function of reducing the structural-soil stiffness ratio distortion and adjusting the weight of the model soil.

2. In theory, the structure-soil stiffness ratio distortion can be completely avoided. However, the practical test involved the limitation of confining pressure and the elasticity of the model soil, and the distortion of the structure-soil stiffness was inevitable. The distortion of the structure-soil stiffness ratio could be reduced as much as possible by adjusting the proportion, which also showed the complexity of the scale model test.

3. In comparison, sawdust soil and sawdust sand could better simulate the original soil, and the effect of the rubber powder soil and sawdust was the worst; therefore, sawdust soil and sawdust sand were applied in the actual vibration table test.

The test conditions and some rebound characteristics of the model soil were limited, which resulted in the connection between the dynamic triaxial test data and the test data of the resonance column not being ideal. At the same time, more tests need to be conducted under different confining pressures so that the hypothesis of determining the shear modulus of soil under small confining pressure by the method of linear interpolation mentioned in this study can be verified or modified. Furthermore, if possible, the bending element should be employed in the shaking model test to record the shear wave in model soil directly, and then soil shear modulus can be obtained by shear velocity and density. This can help to determine the soil properties correctly. These links need to be further improved in follow-up research.

**Author Contributions:** Z.M.: Investigation, Project administration, Data curation, Writing—original draft. G.W.: Methodology, Resource, Supervision, Writing—review and editing. Y.W.: Investigation, Validation, Formal analysis, Visualization. All authors have read and agreed to the published version of the manuscript.

**Funding:** This research work was supported by the National Natural Science Foundation of China (Grant No. 52078386, 51878529, 51678465).

**Data Availability Statement:** Data will be made available on request.

**Conflicts of Interest:** The authors declare that they have no known competing financial interest or personal relationships that could appear to influence the work reported in this paper.

## References

1. Huo, H.; Bobet, A.; Fernández, G.; Ramírez, J. Load transfer mechanisms between underground structure and surrounding ground: Evaluation of the failure of the Daikai Station. *J. Geotech. Geoenvironmental Eng.* **2005**, *131*, 1522–1533. [[CrossRef](#)]
2. Wang, J.N. *Seismic Design of Tunnels: A Simple State of the Art Design Approach*; Parsons Brinckerhoff Inc.: New York, NY, USA, 1993.
3. Ma, X.; Wang, G.; Wu, J.; Ji, Q. Experimental study on the seismic response of subway station in soft ground. *J. Earthq. Tsunami* **2017**, *11*, 1750020. [[CrossRef](#)]
4. Chen, Z.; Chen, W.; Li, Y.; Yuan, Y. Shaking table test of a multi-story subway station under pulse-like ground motions. *Soil Dyn. Earthq. Eng.* **2016**, *82*, 111–122. [[CrossRef](#)]
5. Chen, Z.; Shen, H. Dynamic centrifuge tests on isolation mechanism of tunnels subjected to seismic shaking. *Tunn. Undergr. Space Technol.* **2014**, *42*, 67–77. [[CrossRef](#)]
6. Liu, X.M.; Sheng, Q.; Chen, J.; Ke, W.H.; Yang, J.H. Seismic shaking table test for large-scale underground cavern group (I): Proportioning test on similar materials of surrounding rock. *Rock Soil Mech.* **2015**, *36*, 83–88. (In Chinese)
7. Kitada, Y.; Hirotsu, T.; Iguchi, M. Models test on dynamic structure–structure interaction of nuclear power plant buildings. *Nucl. Eng. Des.* **1999**, *192*, 205–216. [[CrossRef](#)]
8. Turan, A.; Hinchberger, S.D.; El Naggar, H. Design and commissioning of a laminar soil container for use on small shaking tables. *Soil Dyn. Earthq. Eng.* **2009**, *29*, 404–414. [[CrossRef](#)]
9. Moss, R.E.S.; Crosariol, V.; Kuo, S. Shake table testing to quantify seismic soil-structure interaction of underground structures. In Proceedings of the Fifth International Conference on Recent Advances in Geotechnical Earthquake Engineering and Soil Dynamics, San Diego, CA, USA, 24–29 May 2010.
10. Tabatabaiefar, S.H.R.; Fatahi, B.; Samali, B. Numerical and experimental investigations on seismic response of building frames under influence of soil-structure interaction. *Adv. Struct. Eng.* **2014**, *17*, 109–130. [[CrossRef](#)]

11. Hokmabadi, A.S.; Fatahi, B.; Samali, B. Physical modeling of seismic soil-pile-structure interaction for buildings on soft soils. *Int. J. Geomech.* **2015**, *15*, 04014046. [[CrossRef](#)]
12. Pistolas, G.A.; Anastasiadis, A.; Ptilakis, K. Dynamic Behaviour of Granular Soil Materials Mixed with Granulated Rubber: Effect of Rubber Content and Granularity on the Small-Strain Shear Modulus and Damping Ratio. *Geotech. Geol. Eng.* **2018**, *36*, 1267–1281. [[CrossRef](#)]
13. El-Sherbiny, R.M.; Ramadan, S.H.; El-Khouly, M.A. Dynamic properties of sand-EPS bead mixtures. *Geosynth. Int.* **2018**, *25*, 456–470. [[CrossRef](#)]
14. Yan, X.; Yu, H.; Yuan, Y.; Yuan, J. Multi-point shaking table test of the free field under non-uniform earthquake excitation. *Soils Found.* **2015**, *55*, 985–1000. [[CrossRef](#)]
15. Wang, G.; Yuan, M.; Miao, Y.; Wu, J.; Wang, Y. Experimental study on seismic response of underground tunnel-soil-surface structure interaction system. *Tunn. Undergr. Space Technol.* **2018**, *76*, 145–159. [[CrossRef](#)]
16. Zhu, Z.; Zhang, F.; Dupla, J.-C.; Canou, J.; Foerster, E.; Peng, Q. Assessment of tamping-based specimen preparation methods on static liquefaction of loose silty sand. *Soil Dyn. Earthq. Eng.* **2021**, *143*, 106592. [[CrossRef](#)]
17. Bedr, S.; Mezouar, N.; Verrucci, L.; Lanzo, G. Investigation on shear modulus and damping ratio of Algiers marls under cyclic and dynamic loading conditions. *Bull. Eng. Geol. Environ.* **2019**, *78*, 2473–2493. [[CrossRef](#)]
18. Hardin, B.O.; Drnevich, V.P. Shear modulus and damping in soils: Design equations and curves. *J. Soil Mech. Found. Div.* **1972**, *98*, 667–692. [[CrossRef](#)]
19. Hardin, B.O.; Drnevich, V.P. Shear modulus and damping in soils: Measurement and parameter effect. *J. Soil Mech. Found. Div.* **1972**, *98*, 603–624. [[CrossRef](#)]
20. Zhuang, H.; Hu, Z.; Wang, X.; Chen, G. Seismic responses of a large underground structure in liquefied soils by FEM numerical modelling. *Bull. Earthq. Eng.* **2015**, *13*, 3645–3668. [[CrossRef](#)]
21. Clough, R.W.; Penzien, J. *Dynamics of Structures*, 3rd ed.; McGraw-Hill: New York, NY, USA, 1995.

**Disclaimer/Publisher’s Note:** The statements, opinions and data contained in all publications are solely those of the individual author(s) and contributor(s) and not of MDPI and/or the editor(s). MDPI and/or the editor(s) disclaim responsibility for any injury to people or property resulting from any ideas, methods, instructions or products referred to in the content.